Dependence of the coherence spike on the material dephasing time in pump–probe experiments

Michael W. Balk and Graham R. Fleming

Citation: The Journal of Chemical Physics **83**, 4300 (1985); doi: 10.1063/1.449042
View online: http://dx.doi.org/10.1063/1.449042
View Table of Contents: http://scitation.aip.org/content/aip/journal/jcp/83/9?ver=pdfcov
Published by the AIP Publishing

Dependence of the coherence spike on the material dephasing time in pump–probe experiments

Michael W. Balk and Graham R. Fleming
Department of Chemistry and The James Franck Institute, The University of Chicago, Chicago, Illinois 60637

(Received 14 December 1984; accepted 17 July 1985)

The coherence spike observed in the transmitted probe intensity decay curve in pump–probe experiments is analyzed with a model which depends explicitly upon the population decay and dephasing rate constants. Using this model and simple pulse shape functions a series of decay curves are calculated throughout the range of wide to narrow pulse widths relative to the dephasing time. These calculations suggest that the coherence spike may be used to obtain information about the phase coherence in the electronic or vibrational transition being investigated, when the pulse width is comparable to or smaller than the dephasing time. Methods of extracting T_2 from the coherence spike are also discussed.

I. INTRODUCTION

The pump–probe technique has become a standard method for measuring ultrafast population relaxation times. When the pump and probe pulses are created from the same laser pulse, their mutual coherence may give rise to what has been termed the coherence spike, which often shows up in the probe intensity decay curve as a narrow peak centered near zero delay time. Although the presence of the coherence spike complicates the extraction of population relaxation times from the decay curve,[1–6] it has been suggested that the coherence spike may be used as a means to study the coherence properties of laser pulses.[2] The purpose of this manuscript is to show how the coherence spike may be used to extract molecular information. Two recent papers have dealt with methods of removing the coherence spike contribution in order to extract accurate population decay rates in experiments near the limit of the experimental time resolution.[6,7]

The gain in transmitted probe intensity due to the mutual coherence of the pump and probe pulses has been explained, for the case of crossed beam geometry, in terms of a spatial variation in the excited state population (and possibly dipole orientation), induced by the interference of the pump and probe fields where they overlap in the sample.[2,5] This spatial variation acts as a diffraction grating which can scatter pump photons into the probe direction, thus enhancing the detected probe intensity near zero delay time. Coherent coupling between the pump and probe is also possible even if they propagate collinearly through the sample. Though no spatial gratings result in this geometry, a coherence spike still occurs in the transmitted probe field, due to cooperative bleaching of the sample while the pump and probe pulses remain mutually coherent.[6] These are not the only mechanisms, however, which may contribute to the coherence spike. Eichler, Langhans, and Massmann[2] suggest several other mechanisms, such as nonresonant degenerate four-wave mixing in the solvent, besides the coherent coupling mechanisms mentioned above. Recently Palfrey and Heinz[8] have shown that a phase grating, resulting from a modulation in the refractive index, may also affect the shape of the coherence spike when nontransform limited pulses are used. A major difference of the effect of the phase grating compared with that of the amplitude gratings is that the phase grating contribution to the probe signal is antisymmetric with respect to the delay time of the probe pulse. This may be important in the analysis of the probe decay curve in the vicinity of zero delay time. Previous discussions of the coherence coupling effect have assumed that the dephasing time of the transition being pumped is rapid compared with the pulse duration. For picosecond excitation of electronic transitions in solution this is a safe assumption, since electronic dephasing usually occurs on a tens of femtoseconds time scale.[9] However, with the development of pulses as short as 12 fs[10–14] it should be possible to observe the coherence spike on a time scale shorter than, or comparable to, the dephasing time. It is now possible to generate picosecond duration tunable infrared pulses[15,16] and a ground state recovery experiment on the vibrations of hydroxyl groups chemisorbed to colloidal silica has been carried out.[17] In these experiments the vibrational dephasing is the relevant quantity and may be longer than the pulse duration.[18] In this paper we show how the coherence spike can provide information about phase coherence in the transition under investigation.

The sensitivity of the coherence spike to the value of T_2 depends upon the time resolution Δt (intensity FWHM) of the experiment. This sensitivity may be examined by observing the effect on the shape of the coherence spike as $T_2/\Delta t$ is varied. We have performed such an analysis by calculating a sequence of probe decay curves for a range of values of $T_2/\Delta t$. These calculations, discussed in Sec. III (transform limited pulses only), are based on a model for the probe decay curve derived from the third-order perturbation solution of the density matrix equation.[19] The solution of the density matrix equation via perturbation methods has been discussed in the literature by a number of authors.[20] Most notable is the work on four-wave mixing by Ye and Shen,[21] which is based on the well-known diagrammatic approach of Yee and Gustafson.[22] More recently Mukamel has developed a nonimpact (non-Markovian) theory of four-wave mixing.[19,23] A general non-Markovian approach to nonlinear optical phenomena associated with ultrafast relaxation in condensed matter has been discussed by Aihara.[24] All of these approaches yield expressions for $P^{(3)}$, the third order induced polarization of the material system. The response of the system to the incident electric fields is contained in $P^{(3)}$, which determines the nature of the output fields. In view of

 0021-9606/85/214300-08$02.10

the extensive treatment of this topic in the literature, we shall not review the details of the derivation of $P^{(3)}$ from the perturbation expansion of the density matrix. Instead, in Sec. II we discuss only the nature of the approximations introduced into a general expression[19] for $P^{(3)}$ which ultimately lead to an equation for the probe decay curve in which the population and dephasing rate constants appear explicitly [Eqs. (2.10)]. An understanding of the nature of these approximations is essential in order to properly determine the degree to which the model may apply to a given experiment.

One of these approximations concerns the manner in which the model accounts for inhomogeneous broadening. We shall assume that there is a continuous distribution for the average transition frequency (i.e., an average over the temporal fluctuations) of the transition under study and that this distribution is time independent.[9] This constitutes the static contribution to the inhomogeneous broadening. There is also a dynamic contribution originating in the local density fluctuations about each absorber molecule. The density fluctuations create fluctuations in the force exerted by the local environment upon the absorber which in turn result in fluctuations of the transition frequency about its average value. The transition frequency fluctuations are a major part of the dephasing mechanism and hence, their statistical properties are reflected in the value of T_2. These properties are taken into account in the decay curve model through the Markovian approximation discussed in Sec. II [see Eq. (2.7)]. The homogeneous limit to the line broadening results if the distribution of the average transition frequency is a delta function. In general, line broadening in liquids ranges continuously from the limit of homogeneous to inhomogeneous broadening. Between these two limits one encounters the effects of spectral diffusion,[26] which may be defined as the process where the diffusion of molecules in the liquid causes a stochastic shift in the transition frequency, i.e., the distribution of the average transition frequency becomes time dependent. For the sake of simplicity we shall assume that the time scale of dephasing or of the experiment under consideration is sufficiently fast so that spectral diffusion need not be included in the model.

Under these conditions we show, at least in principle, that the value of T_2 can be extracted from the coherence spike provided that a sufficiently high time resolution is used. One might do this, for example, by fitting a model of the decay curve [e.g., Eq. (3.1) or (3.2)] to the experimental data. Both the population decay rates and dephasing rate are treated as curve fitting parameters. If the population decay is relatively slow, then we can obtain the population decay rates first by just fitting the long τ region. As is well-known, this part of the decay curve has the form of a convolution of the population response (e.g., a sum of exponentials) with the pulse autocorrelation function. If the population decay is fast, then a different procedure[6,7] must be used to obtain the population decay rates. It seems natural to conclude that the incoherent population relaxation contribution near $\tau = 0$ would be removed by subtracting this convolution from the entire decay curve. The coherence spike would then remain. We show in Sec. III that this is not rigorously correct when T_2 is of the order of Δt or larger. A more severe problem with the curve fitting method arises from the fact that the shape of the coherence spike depends upon the shape of the pulse envelope. Thus, one must first know the pulse shape in order to construct the appropriate model to fit to the data. Unfortunately, the shape of the envelope of the pulse amplitude cannot be determined by direct measurement. Although pulse shapes can be deduced in principle from intensity autocorrelation measurements, such a procedure is generally not very accurate since different pulse shapes (e.g., Gaussian and sech^2) may have very similar autocorrelation functions. An alternate procedure employing a three pulse scattering technique has been suggested recently by Weiner and Ippen.[27] This method has the advantage that one only need know the electric field autocorrelation rather than the pulse shape. Finally, in Sec. III we suggest the possibility of estimating T_2 from the variation of intensity with pulse width in the coherence spike region.

II. THIRD ORDER TRANSMITTED PROBE INTENSITY FOR A THREE LEVEL SYSTEM

The transmitted intensity of the probe may be divided into two contributions. The first depends only on the probe field alone, and is due to linear transmission and self-modulation.[1] Since this contribution is delay time (τ) independent, it is not important to our discussion here. The second contribution arises from the nonlinear interaction between the pump and probe fields in the material system. We shall assume that both the pump and probe fields are sufficiently weak so that the perturbation expansion of the transmitted probe intensity in the applied fields may be truncated at third order. Since we shall treat here only isotropic material systems, all second order contributions vanish.[28]

We wish to focus in this paper on the temporal rather than the spatial coherence properties of the radiation–matter interaction which gives rise to the coherence spike. For this reason we shall henceforth assume that the sample is sufficiently dilute (e.g., the transmitted probe intensity is approximately a linear function of the absorber concentration) so that coherent propagation effects may be neglected.[5,8] Following Vardeny and Tauc,[1] the change in the transmitted probe intensity due to the interaction of the material system with the pump field is given by the following equation:

$$\Delta I = \frac{\Delta z}{2S} \int ds \int_{-\infty}^{\infty} dt \, \mathrm{Re}[\mathbf{E}^*(\Delta z, t) \cdot i\omega \mathbf{P}^{(3)}(\Delta z, t)]. \quad (2.1)$$

The two integrals in this equation account for the fact that experimentally one measures the intensity integrated over the pulse duration and averaged over the surface area S of the interaction region. E and $P^{(3)}$ are the complex slowly varying parts (slowly varying envelope approximation[29]) of the total applied electric field and the third order induced polarization, respectively, and Δz is the path length.

Since we wish to examine the effect on the coherence spike as Δt approaches T_2, we require an expression for $P^{(3)}$ which depends explicitly upon T_2. Earlier studies[1,5] of the coherence spike considered only the case $\Delta t \gg T_2$, so that the shape of the coherence spike was not expected to depend upon the explicit value of T_2. Hence, the models of the probe decay curve employed in those studies did not contain T_2

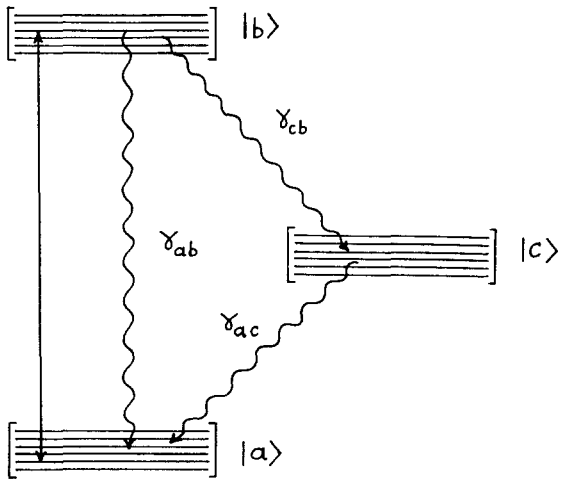

FIG. 1. Three level model of material system transitions. The solid line denotes pump and probe induced transitions, and the wavy lines denote relaxation pathways. Each path is labeled by its rate constant.

except in an overall scale factor which of course does not affect the *shape* of the curve. The pump–probe technique is one of many variations of four-wave mixing (4WM), which has been treated by a number of authors.[30] The time-dependent perturbation calculation of $P^{(3)}$ has been discussed with regard to virtually all forms of 4WM (see Sec. I) and hence, we shall only briefly discuss the relevant approximations used in the calculation of $P^{(3)}$ that are important to the development of our final expression for the probe decay curve [Eq. (2.10)]. In this expression T_2 appears explicitly and affects the shape of the coherence spike as long as the value T_2 is comparable or larger than Δt. We shall show below that our expression for ΔI tends towards the rapid dephasing form derived previously when we let $T_2/\Delta t \to 0$.

The chemical system dynamics are modeled by the radiative and nonradiative transitions within the effective three level system shown in Fig. 1. $|a\rangle$ denotes a submanifold of vibronic levels in the ground electronic state, $|b\rangle$ is a submanifold connected to $|a\rangle$ by the pump and probe fields, and $|c\rangle$ is a set of reservoir levels. The three level model is used in a standard third order perturbation calculation[21] yielding the following expression for $P^{(3)}$:

$$\begin{aligned} P^{(3)}(\mathbf{r},t,\Delta) = & -\frac{i}{\hbar^3}\int_{-\infty}^{t} dt_1 \int_{-\infty}^{t_1} dt_2 \int_{-\infty}^{t_2} dt_3 \\ & \times \{ \langle M^I_{ab;i}(t-t_3) M^I_{ba;j}(t_1-t_3) M^I_{ab;k}(t_2-t_3) M^I_{ba;l}(0)\rangle_B \\ & \times \exp[-(\tfrac{1}{2}\gamma_b - i\Delta)(t-t_1+t_2-t_3)]\hat{I}(t_1-t_2) \\ & \times E_j(\mathbf{r},t_1) E^*_k(\mathbf{r},t_2) E_l(\mathbf{r},t_3) + \langle M^I_{ab;i}(t-t_3) \\ & \times M^I_{ba;j}(t_1-t_3) M^I_{ba;k}(t_2-t_3) M^I_{ab;l}(0)\rangle_B \\ & \times \exp[-(\tfrac{1}{2}\gamma_b - i\Delta)(t-t_1) - (\tfrac{1}{2}\gamma_b + i\Delta)(t_2-t_3)] \\ & \times \hat{I}(t_1-t_2) E_j(\mathbf{r},t_1) E^*_l(\mathbf{r},t_2) E_k(\mathbf{r},t_3)\}. \end{aligned} \tag{2.2}$$

There is an implied sum in this equation over the repeated Cartesian indices j, k, and l, and $\gamma_b \equiv \gamma_{cb} + \gamma_{gb}$ is the total rate of population loss from $|b\rangle$. The function $\hat{I}(t)$ is defined by

$$\hat{I}(t) = A\exp[-\gamma_b t] + B\exp[-\gamma_{ac} t], \tag{2.3}$$

where

$$A = 2 - B; \quad B = \gamma_{cb}/(\gamma_b - \gamma_{ac}). \tag{2.4}$$

Note that $\hat{I}(t)$ does *not* have a singularity at $\gamma_b = \gamma_{ac}$. Rather, it is straightforward to show that

$$\lim_{\gamma_{ac}\to\gamma_b} \hat{I}(t) = (2+\gamma_{cb}t)\exp[-\gamma_b t]. \tag{2.5}$$

The difference between the band center frequency of the laser pulse ω and the transition frequency ω_0 is

$$\Delta = \omega - \omega_0. \tag{2.6}$$

Consequently, the static contribution to the inhomogeneous broadening discussed in the Introduction may be accounted for by averaging Eq. (2.2) over the distribution $g(\Delta)$ of Δ values,[9,34] i.e., over the distribution of ω_0.

The dynamic contribution to the inhomogeneous broadening arising from the stochastic fluctuations of ω_0 (see Sec. I) is contained in the four point time correlation function[19] of the electric moment density M. The superscript "I" on M in Eq. (2.2) denotes an interaction picture defined by the thermal bath degrees of freedom[19] and $\langle\cdots\rangle_B$ is the corresponding ensemble average. In order to obtain an analytic function for ΔI which depends explicitly on T_2, we have employed the semiclassical weak-coupling Markovian approximation[19] to the four point time correlation function:

$$\begin{aligned} & \langle M^I_{ab;i}(t-t_3) M^I_{ba;j}(t_1-t_3) M^I_{ab;k}(t_2-t_3) M^I_{ba;l}(0)\rangle_B \\ & \approx N\langle \mu_{ab;i}\mu_{ba;j}\mu_{ab;k}\mu_{ba;l}\rangle_B \exp[-\hat{\Gamma}_{ab}(t-t_1+t_2-t_3)], \end{aligned} \tag{2.7}$$

where N is the absorber particle density, μ is the dipole operator for a single absorber, and $\hat{\Gamma}_{ab}$ is the pure dephasing rate for $|a\rangle \leftrightarrow |b\rangle$ transitions. The weak coupling aspect of this approximation involves only the reasonable assumption that the dipole operator varies little with the bath degrees of freedom. The Markovian approximation assumes that the bath has a short correlation time relative to $2\pi/\hat{\Gamma}_{ab}$. This condition is probably fulfilled for vibrational dephasing on a picosecond or longer time scale, but it is less certain whether $\hat{\Gamma}_{ab}$ and thus T_2 is well defined for electronic dephasing on the tens of femtoseconds time scale.[24]

Electronic dephasing on this time scale has been observed in recent experiments on several dye solutions.[9] To the extent that molecular collisions are a major mechanism of dephasing, one might expect to observe electronic dephasing on a longer time scale in systems composed of uncharged absorbers. The time scale might also be lengthened by increasing the solvent viscosity. In that case, the study of electronic dephasing in liquids as a function of applied pressure should be very interesting.

We now specialize to the case in which the pump and probe have parallel polarization, are transform limited and cross each other with a small angle inside the sample. If the x axis lies along the polarization direction, then only $P^{x(3)}(r,t,\Delta)$ is nonzero. The total incident field amplitude is the sum of the pump (subscript "1") and the probe (subscript "2") amplitudes:

$$\mathbf{E}(\mathbf{r},t;\tau) = \mathbf{E}_1(\mathbf{r},t)\exp[i\mathbf{k}_1\cdot\mathbf{r}] + \mathbf{E}_2(\mathbf{r},t;\tau)\exp[i\mathbf{k}_2\cdot\mathbf{r}], \tag{2.8}$$

where τ is the relative delay time between the pump and probe pulses. In the manner of Vardeny and Tauc[1] we shall assume that the probe is a weaker delayed image of the pump:

$$|\mathbf{E}_2(\mathbf{r},t;\tau)| = b\,|\mathbf{E}_1(\mathbf{r},t-\tau)|; \quad b<1. \tag{2.9}$$

Substituting Eqs. (2.7)–(2.9) into Eq. (2.2) and the result into Eq. (2.1), the spatial averaging is then performed exactly as described earlier.[1] The result is that only two types of field amplitude products survive in the expression for ΔI. In terms of the subscripts 1 and 2, these products may be denoted by 2211 and 2112, whose contributions to ΔI are conventionally labeled γ and β, respectively. The results of the spatial averaging in Eq. (2.1) may be given in scaled form as follows:

$$\Delta I_s(\tau,\Delta) \equiv \frac{2\hbar^3}{N\langle|\mu_{ab;x}|^4\rangle\omega\Delta z b^2}\,\Delta I(\tau,\Delta)$$
$$\equiv \gamma_S^A(\tau,\Delta)+\gamma_S^B(\tau,\Delta)+\beta_S^A(\tau,\Delta)+\beta_S^B(\tau,\Delta), \tag{2.10a}$$

where

$$\gamma_S^A(\tau,\Delta) = \mathrm{Re}\int_{-\infty}^{\infty} dt \int_{-\infty}^{t} dt_1 \int_{-\infty}^{t_1} dt_2 \int_{-\infty}^{t_2} dt_3\, \hat{I}(t_1-t_2) \times\exp[-\Gamma_{ab}(t-t_1+t_2-t_3)] \times E_1^*(t-\tau)E_1(t_1-\tau)E_1^*(t_2)E_1(t_3), \tag{2.10b}$$

$$\gamma_S^B(\tau,\Delta) = \mathrm{Re}\int_{-\infty}^{\infty} dt \int_{-\infty}^{t} dt_1 \int_{-\infty}^{t_1} \mathrm{d}t_2 \int_{-\infty}^{t_2} dt_3\, \hat{I}(t_1-t_2) \times\exp[-\Gamma_{ab}(t-t_1)-\Gamma_{ab}^*(t_2-t_3)] \times E_1^*(t-\tau)E_1(t_1-\tau)E_1^*(t_3)E_1(t_2), \tag{2.10c}$$

$$\beta_S^A(\tau,\Delta) = \mathrm{Re}\int_{-\infty}^{\infty} dt \int_{-\infty}^{t} dt_1 \int_{-\infty}^{t_1} dt_2 \int_{-\infty}^{t_2} dt_3\, \hat{I}(t_1-t_2) \times\exp[-\Gamma_{ab}(t-t_1+t_2-t_3)] \times E_1^*(t-\tau)E_1(t_1)E_1^*(t_2)E_1(t_3-\tau), \tag{2.10d}$$

$$\beta_S^A(\tau,\Delta) = \mathrm{Re}\int_{-\infty}^{\infty} dt \int_{-\infty}^{t} dt_1 \int_{-\infty}^{t_1} dt_2 \int_{-\infty}^{t_2} dt_3\, \hat{I}(t_1-t_2) \times\exp[-\Gamma_{ab}(t-t_1)-\Gamma_{ab}^*(t_2-t_3)] \times E_1^*(t-\tau)E_1(t_1)E_1^*(t_3)E_1(t_2-\tau), \tag{2.10e}$$

and

$$\Gamma_{ab} \equiv \Gamma_{ab}^0 - i\Delta, \tag{2.11}$$

where Γ_{ab}^0 is the total dephasing rate,

$$\Gamma_{ab}^0 \equiv \hat{\Gamma}_{ab} + \tfrac{1}{2}\gamma_b = 2\pi/T_2. \tag{2.12}$$

In order to examine the effects of phase coherence in ΔI_s, we have evaluated Eqs. (2.10) for a range of values of $T_2/\Delta t$ for two simple model pulse shapes. The results of these calculations are discussed in Sec. III.

The pulse shapes used were the single-sided exponential (exp1) and symmetric double-sided exponential (exp2s):

$$\exp[-(\ln 2/2\Delta t)t\,]\theta(t); \quad \text{exp1}, \tag{2.13}$$

$$\exp[(\ln 2/\Delta t)t\,]\theta_>(-t) + \exp[-\ln 2/\Delta t)t\,]\theta(t); \quad \text{exp2}s \tag{2.14}$$

($\theta_>(t)=0$ if $t\leqslant 0$, and 1 if $t>0$). While these functions may only crudely represent real pulse shapes, their use permits the integrals to be evaluated analytically. The choice of exp1 was also motivated by the fact that it has been used in the previous work for the case $T_2/\Delta t\to 0$[1,2]. However, exp1 undergoes a sudden change in amplitude from unity to zero at $t=0$, which tends to violate the slowly varying envelope approximation used in Eq. (2.1). This is not the case with the exp2s pulse shape.

Before concluding this section we will show how our expression for ΔI_s [Eqs. (2.10)] may be transformed in the limit $T_2/\Delta t\to 0$ into a form similar to that derived by Vardeny and Tauc.[1] This limit is equivalent to letting $\Gamma_{ab}^0\to\infty$ in Eqs. (2.10), and amounts to replacing $\exp[-\Gamma_{ab}(t-t_1+t_2-t_3)]$ by $Q\delta(t-t_1)\delta(t_2-t_3)$, where Q is a constant. The result is

$$\gamma_S^A(\tau)+\gamma_S^B(\tau)\to\gamma_S^0(\tau) = \mathrm{Re}\int_{-\infty}^{\infty} dt \int_{-\infty}^{\infty} dt_1 \times|E_1(t-\tau)|^2 A(t-t_1)|E_1(t_1)|^2; \quad \Gamma_{ab}^0\to\infty, \tag{2.15a}$$

$$\beta_S^A(\tau)+\beta_S^B(\tau)\to\beta_S^0(\tau) = \mathrm{Re}\int_{-\infty}^{\infty} dt \int_{-\infty}^{\infty} dt_1\, E_1^*(t-\tau)E_1(t)A(t-t_1) \times E_1^*(t_1)E_1(t_1-\tau); \quad \Gamma_{ab}^0\to\infty, \tag{2.15b}$$

where

$$A(t-t_1) = 2Q\hat{I}(t-t_1)\theta(t-t_1). \tag{2.15c}$$

The function $A(t)$ describes the material response of the system and depends only upon population relaxation rates. Apart from terms related to molecular diffusion, Eqs. (2.15) are also similar to expressions developed by Wherett and coworkers[5] where again, the limit $T_2/\Delta t\to 0$ was assumed.

III. MODEL CALCULATIONS OF PHASE COHERENCE EFFECTS IN $\Delta I_s(\tau)$

Substituting Eq. (2.13) or (2.14) into Eq. (2.10) and performing the integrations yields an analytic model for $\Delta I_s(\tau,\Delta)$. We shall discuss the results of calculations based on this model for the case of a homogeneously broadened system in the sense that all the absorbing molecules have the same average transition frequency ω_0 on the time scale of the experiment. We then assume that the laser band center frequency is tuned to ω_0 so that $\Delta=0$. While T_2 may be extracted simply from the absorption linewidth in the case of homogeneous broadening, it turns out that when inhomogeneous broadening is included in the manner outlined above, only relatively minor changes in the shape of the coherence spike result. The important point is that the same general trend in the behavior of the coherence spike as $T_2/\Delta t$ is varied is observed both for homogeneous and inhomogeneous broadening (the laser band center frequency is tuned to ω_0 or $\langle\omega_0\rangle_{g(\omega_0)}$), respectively.

If we substitute the exp1 pulse shape [Eq. (2.13)] into

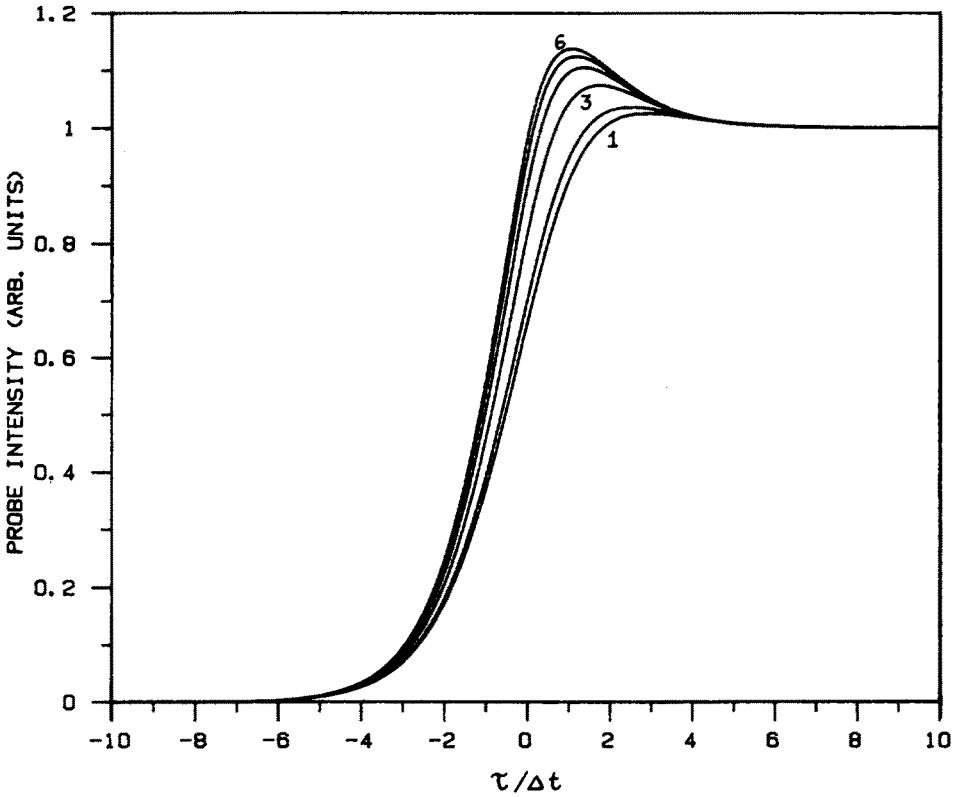

FIG. 2. Probe decay curves for the exp2*s* pulse shape [Eq. (2.32)]. The six curves correspond to the six values of $T_2/\Delta t$ appearing in Table I.

Eqs. (2.10), the result is a sum of exponentials for both $\gamma_s = \gamma_S^A + \gamma_S^B$ and $\beta_S = \beta_S^A + \beta_S^B$:

$$\gamma_s(\tau) = 2[\Lambda_1 + \Lambda_2]\exp(2\sigma\tau)\theta_>(-\tau) + \{\Lambda_3 \exp[-(\Gamma_{ab}^0 + \sigma)\tau] + \Lambda_4 \exp[-2\sigma\tau] + \Lambda_5 \exp[-\gamma_b\tau] + \Lambda_6 \exp[-\gamma_{ac}\tau]\}\theta(\tau); \quad \text{exp1}, \tag{3.1a}$$

$$\beta_S(\tau) = [2\Lambda_1 + \Lambda_2]\exp(-2\sigma|\tau|) + \Lambda_2 \exp[(-\Gamma_{ab}^0 + \sigma)|\tau|]; \quad \text{exp1}, \tag{3.1b}$$

where

$$\sigma \equiv (\ln 2)/2\Delta t; \quad \text{exp1}. \tag{3.1c}$$

The Λ coefficients are functions of the inverse pulse width σ, the population rate constants, and the dephasing rate Γ_{ab}^0. Since each coefficient is a different function of Γ_{ab}^0, each term in γ_s and β_s is generally expected to contribute to the phase coherence effects in ΔI_s, rather than just the terms proportional to $\exp[-(\Gamma_{ab}^0 + \sigma)\tau]$.

TABLE I. Rate constants for the model calculations of ΔI_s.[a]

Curve	$T_2/\Delta t$	$\gamma_b \cdot \Delta t$	$\gamma_{cb} \cdot \Delta t$	$\gamma_{ac} \cdot \Delta t$
1	5.0	1.0×10^{-4}	5.0×10^{-5}	5.0×10^{-5}
2	4.0	1.0×10^{-4}	5.0×10^{-5}	5.0×10^{-5}
3	2.0	1.0×10^{-4}	5.0×10^{-5}	5.0×10^{-5}
4	1.0	1.0×10^{-4}	5.0×10^{-5}	5.0×10^{-5}
5	0.5	1.0×10^{-4}	5.0×10^{-5}	5.0×10^{-5}
6	0.2	1.0×10^{-4}	5.0×10^{-5}	5.0×10^{-5}

[a] $\sigma\cdot\Delta t$ is ln 2/2 for exp1, and ln 2 for exp2*s* [see Eqs. (3.1c) and (3.3)].

The corresponding expressions for the exp2*s* pulse shape are

$$\gamma_s(\tau) = 2[G_1 + G_2\tau]\exp(2\sigma\tau)\theta_>(-\tau) + 2\{[G_3 + G_4\tau]\exp(-2\sigma\tau) + [G_5 + G_6\tau] \times \exp(-[\Gamma_{ab}^0 + \sigma]\tau) + G_7 \exp(-\gamma_b\tau) + G_8 \exp(-\gamma_{ac}\tau)\}\theta(\tau); \quad \text{exp2}s, \tag{3.2a}$$

$$\beta_s(\tau) = \{[G_q + G_{10}\tau + G_{11}\exp(\gamma_b\tau) + G_{12}\exp(\gamma_{ac}\tau)]\exp(2\sigma\tau) + G_{13}\exp([\Gamma_{ab}^0 + \sigma]\tau)\}\theta_>(-\tau) + \{[G_{14} + G_{15}\tau + G_{16}\exp(-\gamma_b\tau) + G_{17}\exp(-\gamma_{ac}\tau)]\exp(-2\sigma\tau) + [G_{18} + G_{19}\tau]\exp(-[\Gamma_{ab}^0 + \sigma]\tau)\}\theta(\tau); \quad \text{exp2}s, \tag{3.2b}$$

where

$$\sigma \equiv (\ln 2)/\Delta t; \quad \text{exp2}s. \tag{3.3}$$

The same comments made about the Λ coefficients above also apply to the G coefficients.

Several calculations of ΔI_s using the exp2*s* pulse shape are shown in Fig. 2 for the values of $T_2/\Delta t$ appearing in Table I. These calculations were performed using very small population decay rates so that the coherence peak would be clearly visible. The six curves appearing in Fig. 2 were rescaled to a value of unity at $\tau/\Delta t = 10$. Note that all six curves converge to the same shape of $\tau/\Delta t$ in the region of negligible overlap of the pump and probe. In this region it is straightforward to show that $\Delta I_s(\tau)$ is just the convolution of

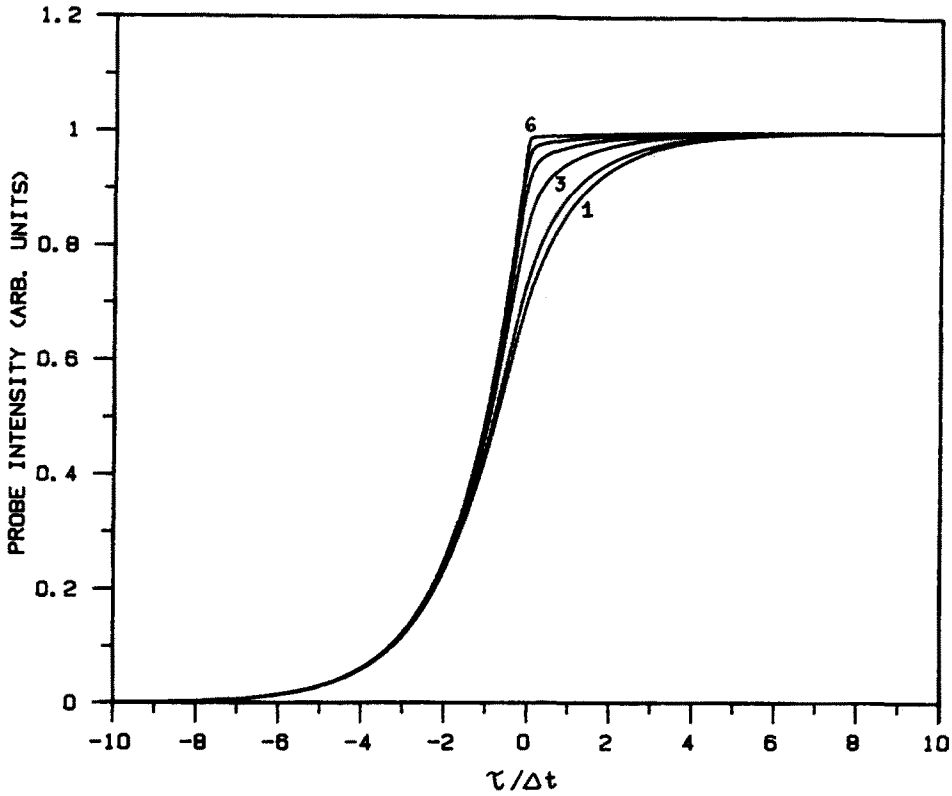

FIG. 3. Probe decay curves for the exp1 pulse shape [Eq. (2.31)]. The six curves correspond to the six values of $T_2/\Delta t$ appearing in Table I.

the pulse intensity autocorrelation function with $A(t)$ [see Eq. (2.15c)].

As $T_2/\Delta t$ increases we see in Fig. 2 that the intensity in the coherence spike region decreases, and the peak shifts away from $\tau = 0$. This trend may be understood qualitatively as follows. If $T_2/\Delta t$ is small, then the magnitude of the total phase coherence tends to follow the envelope of the total (pump plus probe) field amplitude. However, if $T_2/\Delta t$ is large, then that part of the probe which interacts with the sample at $t(t)$ will be affected by the phase coherence generated by the pump at earlier times (for $\tau > 0$) as well. The length of this phase coherence memory increases with $T_2/\Delta t$ resulting in a slower rate of change of $\Delta I_s(\tau)$ with τ near the coherence spike, which in turn forces the peak to appear at larger $\tau/\Delta t$.

The curve with the largest peak in Fig. 2 differs little from the $T_2/\Delta t \to 0$ limit. Thus, the fast dephasing limit is effectively achieved for $\Delta t \gtrsim 5T_2$.

Figure 3 shows the results for the exp1 pulse shape. No definite coherence peak appears. Rather, the rising edge of ΔI_s becomes steeper and a square shoulder appears as $T_2/\Delta t$ decreases. The square shoulder is characteristic of the fast dephasing limit for exp1 pulses [especially when $A(t)$ is a step function],[1] and is also effectively reached when $\Delta t \gtrsim 5T_2$.

While we have examined only two simple pulse shapes, the results discussed above suggest that the following simple algorithm may provide a way to roughly estimate the magnitude of T_2. The variation of intensity in the coherence region may be viewed as a function of Δt for fixed T_2.[31] If a sequence of decay curves can be obtained experimentally by varying the pulse width and measuring ΔI in the coherence region, then the largest value of Δt beyond which no further relative intensity increase can be seen is roughly mT_2. In the case of the model calculations discussed here, m has a value of about 5. The value of m is also about 5 when inhomogeneous broadening is included in the calculations. Further work is required to determine if this simple procedure applies when more realistic pulse shapes, e.g., sech^2, are used, when the pulses are mildly or strongly nontransform limited,[8] and when excited state absorption occurs.

We will conclude this paper with a discussion of the application of a method for isolating the coherence spike, commonly used in the fast dephasing limit, to the case of slow dephasing. We first describe the method for the case of fast dephasing. When $T_2/\Delta t \to 0$, the decay curve has the form

$$\Delta I_s^0(\tau) = \gamma_S^0(\tau) + \beta_S^0(\tau), \tag{3.4}$$

where $\gamma_S^0(\tau)$ and $\beta_S^0(\tau)$ are defined by Eqs. (2.15). Since $\gamma_S^0(\tau)$ may be rigorously recast[1] in the form of a convolution of the pulse intensity autocorrelation function with the population response $A(t)$, it may be calculated, to within a scale factor, from experimental measurements of the intensity autocorrelation and the population decay rates. The $\beta_S^0(\tau)$, which is the coherence spike in the fast dephasing limit, may be obtained by subtracting $\gamma_S^0(\tau)$ from $\Delta I_s^0(\tau)$.

When $T_2/\Delta t > 0$, the decay curve is given by Eqs. (2.10), which may be rigorously rewritten in the form

$$\Delta I_s(\tau) = \Delta I_s^0(\tau) + C_D(\tau), \tag{3.5}$$

where $C_D(\tau)$ may be viewed as a finite dephasing correction. Comparison of Eq. (3.5) with Figs. 2 or 3 shows that $C_D(\tau)$ is negative in the coherence spike region and decreases as $T_2/\Delta t$ increases, while at longer $\tau/\Delta t$, $C_D(\tau)$ is proportional to $\gamma_s^0(\tau)$. The latter property of $C_D(\tau)$ causes a problem to arise related to the rescaling of the experimental quantities

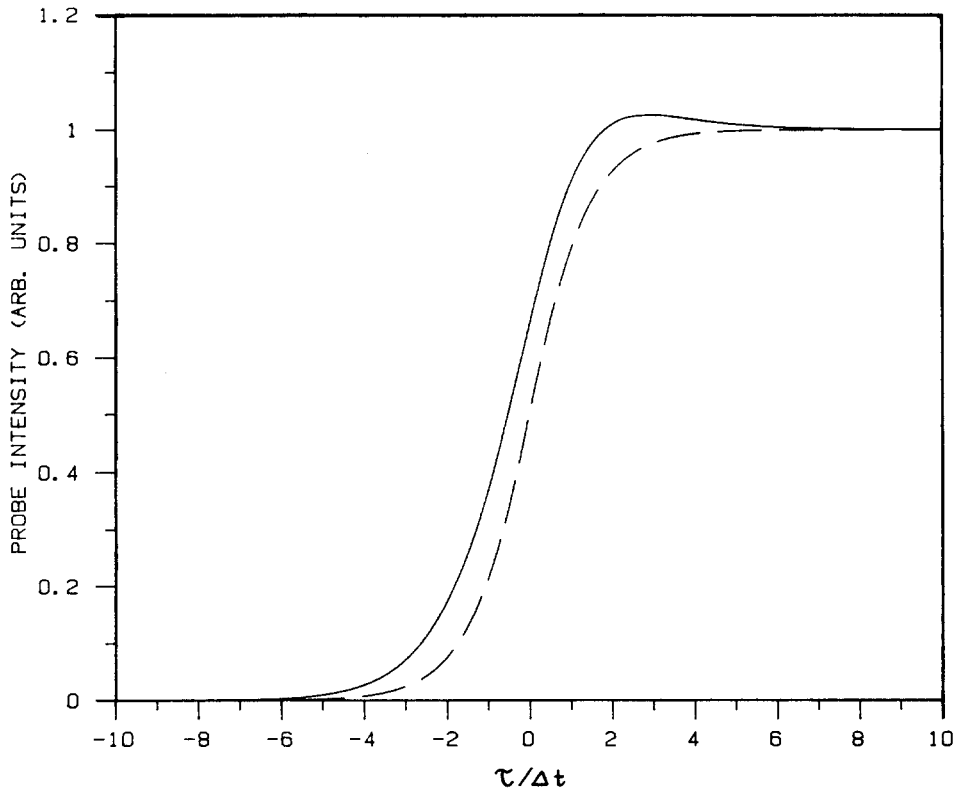

FIG. 4. Decay curve 1 from Fig. 2 (—) together with $\gamma_s^0(\tau)$ [Eq. (2.33a)] (- - -).

$\Delta I(\tau)$ and $\gamma^0(\tau)$ required (so that they superimpose beyond the coherence spike region) before their difference can be obtained. For some value τ_L of the delay time beyond the coherence spike, $\beta^0(\tau \geqslant \tau_L) = 0$. Thus, in the fast dephasing limit, we may rescale $\Delta I^0(\tau)$ as follows:

$$\Delta I_s^{0\dagger}(\tau) \equiv \Delta I^0(\tau)/\Delta I^0(\tau_L) = \gamma_s^{0*}(\tau) + \beta_S^{0*}(\tau), \tag{3.6}$$

where here the asterisks denote division by $\gamma^0(\tau_L)$. Since $\Delta I_s^{0\dagger}(\tau)$ and $\gamma_s^{0*}(\tau)$ can both be measured independently, no scaling problem occurs in the fast dephasing limit, and $\beta_s^{0*}(\tau)$ may be obtained as described above. However, as a consequence of

$$C_D(\tau > \tau_L) = a\gamma_s^0(\tau), \tag{3.7}$$

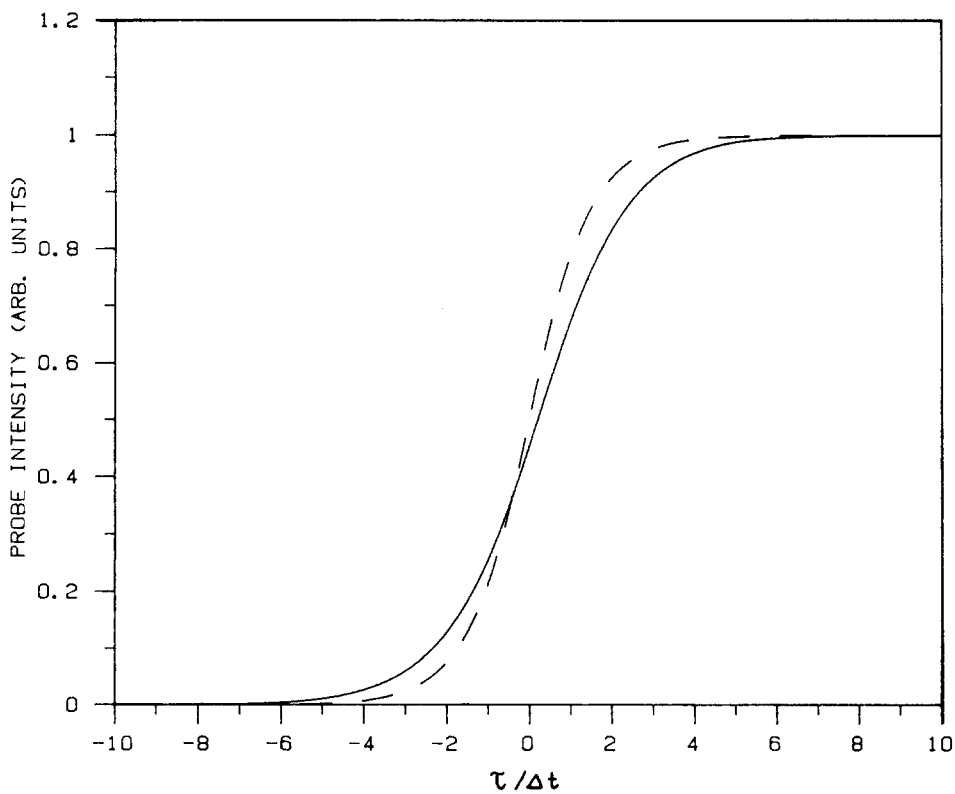

FIG. 5. Probe decay curve (exp2s pulse shape [Eq. (2.32)] for the case $T_2/\Delta t = 20$ (other parameters the same as in Table I) (—), and $\gamma_s^0(\tau)$ [Eq. (2.33a)] (- - -).

we obtain the following rescaled intensity from Eq. (3.5) in the case of slow dephasing:

$$\Delta I_s^{\dagger}(\tau) = \frac{1}{1+a}\left[\gamma_s^{0*}(\tau) + \beta_s^{0*}(\tau) + C_D^{*}(\tau)\right]. \tag{3.8}$$

Since $C_D(\tau)$ cannot be measured directly, the proportionality constant "a" is unknown. If we now subtract the convolution $\gamma_s^{0*}(\tau)$ from the decay curve $\Delta I_s^{\dagger}(\tau)$,

$$\Delta I_s^{\dagger}(\tau) - \gamma_s^{0*}(\tau) = \frac{1}{1+a}\left[-a\gamma_s^{0*}(\tau) + \beta_s^{0*}(\tau) + C_D^{*}(\tau)\right], \tag{3.9}$$

we find in general that $\gamma_s^{0*}(\tau)$ has not been totally removed from $\Delta I_s^{\dagger}(\tau)$, if $a \neq 0$ ($a \equiv 0$ in the fast dephasing limit). Moreover, since $C_D^{*}(\tau)$ tends to be negative near $\tau = 0$, $\Delta I_s^{\dagger}(\tau) - \gamma_s^{0*}(\tau)$ may even acquire negative values in the coherence spike region, i.e., $\Delta I_s^{\dagger}(\tau)$ and $\gamma_s^{0*}(\tau)$ may cross.

In Fig. 4 we have plotted curve 1 from Fig. 3 together with $\gamma_s^{0*}(\tau)$ (both rescaled to unity at $\tau_L = 10\Delta t$). A similar result is obtained for the other curves in Fig. 3. Thus, $\Delta I_s^{\dagger}(\tau)$ and $\gamma_s^{0*}(\tau)$ do not cross even for $T_2/\Delta t$ as large as 5 in the model calculations discussed above. However, crossing eventually occurs at $T_2/\Delta t$ is increased beyond 5 (see Fig. 5). Consequently, we conclude that when $T_2/\Delta t > 0$, subtraction of the convolution $\gamma_s^{0*}(\tau)$ from $\Delta I_s^{\dagger}(\tau)$ is not a rigorous method for isolating the coherence spike, although it may be a reasonable approximation when $T_2/\Delta t$ is small.

ACKNOWLEDGMENTS

We gratefully acknowledge the support of this work by the National Science Foundation. We also thank R. A. Engh for many helpful discussions.

[1]Z. Vardeny and J. Tauc, Opt. Commun. **39**, 396 (1981).
[2]H. J. Eichler, D. Langhans, and F. Massmann, Opt. Commun. **50**, 117 (1984).
[3]E. P. Ippen and C. V. Shank, in *Ultrashort Light Pulses*, edited by S. L. Shapiro (Springer, New York, 1977), p. 83.
[4]A. von Jena and H. E. Lessing, Appl. Phys. **19**, 131 (1979).
[5]B. S. Wherrett, A. L. Smirl, and T. F. Boggess, IEEE J. Quantum Electron. **QE-19**, 680 (1983).
[6]T. F. Heinz, S. L. Palfrey, and K. B. Eisenthal, Opt. Lett. **9**, 359 (1984).
[7]R. A. Engh, J. W. Petrich, and G. R. Fleming, J. Phys. Chem. **89**, 618 (1985).
[8]S. L. Palfrey and T. F. Heinz, J. Opt. Soc. Am. B **2**, 674 (1985).
[9](a) Weiner and Ippen, Ref. 20; A. M. Weiner, S. DeSilvestri, and E. P. Ippen, J. Opt. Soc. Am. B **2**, 654 (1985); (b) T. Yajima and Y. Taira, J. Phys. Soc. Jpn. **47**, 1620 (1979); (c) H. Souma, E. J. Heilweil, and R. M. Hochstrasser, J. Chem. Phys. **76**, 5693 (1982); see also Ref. 25.
[10]J. G. Fujimoto, A. M. Weiner, and E. P. Ippen, Appl. Phys. Lett. **44**, 832 (1984).
[11]J. M. Halbout (private communication).
[12]C. V. Shank, R. L. Fork, R. Yen, R. H. Stolen, and W. J. Tomlinson, Appl. Phys. Lett. **40**, 761 (1982).
[13]B. Nikolaus and D. Grischkowsky, Appl. Phys. Lett. **43**, 228 (1983).
[14]R. L. Fork, B. I. Greene, and C. V. Shank, Appl. Phys. Lett. **38**, 671 (1981).
[15]F. Wondrazek, A. Seilmeier, and W. Kaiser, Chem. Phys. Lett. **104**, 121 (1984).
[16]M. Berg, A. L. Harris, J. K. Brown, and C. B. Harris, Opt. Lett. **9**, 50 (1984).
[17]E. J. Heilweil, M. P. Casassa, R. R. Cavanagh, and J. C. Stephenson, J. Chem. Phys. **81**, 2856 (1984).
[18]A. Laubereau and W. Kaiser, Rev. Mod. Phys. **50**, 607 (1978).
[19]Our model for the probe decay curve is based upon Mukamel's approach to the solution of the Liouville equation for the density matrix: S. Mukamel, Phys. Rev. A **28**, 3480 (1983). See also Refs. 5, 21–24, 28, and 32(b) for examples of other approaches.
[20]For a representative sample, see Refs. 5, 21–24, 28, and 32(b).
[21]P. Ye and Y. R. Shen, Phys. Rev. A **25**, 2183 (1982).
[22]T. K. Yee and T. K. Gustafson, Phys. Rev. A **18**, 1597 (1978).
[23]R. W. Boyd and S. Mukamel, Phys. Rev. A **29**, 1973 (1984); S. Mukamel, Phys. Rep. **93**, 1 (1982).
[24]A. Aihara, Phys. Rev. B **25**, 53 (1982).
[25]J. J. Song, J. H. Lee, and M. D. Levenson, Phys. Rev. A **17**, 1439 (1978).
[26]See, for example, T. Yajima and H. Souma, Phys. Rev. A **17**, 309 (1978).
[27]A. M. Weiner and E. P. Ippen, Opt. Lett. **9**, 53 (1984).
[28]See, for example, M. D. Levenson, *Introduction to Nonlinear Laser Spectroscopy* (Academic, New York, 1982), p. 46.
[29]M. Sargent III, M. O. Scully, and W. E. Lamb, Jr., *Laser Physics* (Addison–Wesley, London, 1974), pp. 198–199.
[30]A representative sample of the work on 4WM is: S. H. J. Druet, J-P. E. Taran, and Ch. J. Borde, J. Phys. (Paris) **40**, 841 (1979); **41**, 183 (1980); J.-L. Oudar and Y. R. Shen, Phys. Rev. A **22**, 1141 (1980); see also Refs. 19–24, 26, and 28.
[31]In case inhomogeneous broadening is present, the set of probe decay curves obtained by fixing T_2 and varying Δt is not in general equivalent to the set of curves produced by fixing Δt and varying T_2.